Accepted Manuscript

Peripheral Quantitative Computed Tomography: Review of Evidence and Recommendations for Image Acquisition, Analysis and Reporting, Among Individuals with Neurological Impairment

Cervinka T , Giangregorio L , Sievanen H , Cheung AM , Craven BC

PII: S1094-6950(18)30065-9
DOI: 10.1016/j.jocd.2018.07.003
Reference: JOCD 1055

To appear in: *Journal of Clinical Densitometry*

Received date: 16 April 2018
Revised date: 7 May 2018
Accepted date: 7 October 2018

Please cite this article as: Cervinka T , Giangregorio L , Sievanen H , Cheung AM , Craven BC , Peripheral Quantitative Computed Tomography: Review of Evidence and Recommendations for Image Acquisition, Analysis and Reporting, Among Individuals with Neurological Impairment, *Journal of Clinical Densitometry* (2018), doi: 10.1016/j.jocd.2018.07.003

Peripheral Quantitative Computed Tomography: Review of Evidence and Recommendations for Image Acquisition, Analysis and Reporting, Among Individuals with Neurological Impairment

Cervinka T[1], Giangregorio L[1,2] , Sievanen H[3], Cheung AM[4,6], Craven BC[1,2,4, 5,6]

[1]Neural Engineering and Therapeutics Team, Toronto Rehabilitation Research Institute – University Health Network, Toronto, Ontario, Canada

[2]Department of Kinesiology, University of Waterloo, Waterloo, Ontario, Canada

[3]Bone Research Group, UKK Institute, Tampere, Finland

[4]Centre of Excellence in Skeletal Health Assessment, University Health Network, Toronto, Ontario, Canada

[5]Brain and Spinal Cord Rehabilitation Program, Toronto Rehabilitation Institute – University Health Network, Toronto, Canada

[6]Department of Medicine, University of Toronto, Toronto, Ontario, Canada

Running title: Recommendations for pQCT assessment

Corresponding author: Cervinka T, Neural Engineering and Therapeutics Team, Toronto Rehabilitation Institute – University Health Network, Toronto, Ontario, Canada, tomas.cervinka@hotmail.com, +1 416 597 3422

ABSTRACT

In 2015, the International Society for Clinical Densitometry (ISCD) position statement regarding peripheral quantitative computed tomography (pQCT) did not recommend routine use of pQCT, in clinical settings until consistency in image acquisition and analysis protocols are reached, normative studies conducted, and treatment thresholds identified. To date, the lack of consensus-derived recommendations regarding pQCT implementation remains a barrier to implementation of pQCT technology.

Thus, based on description of available evidence and literature synthesis, this review recommends the most appropriate pQCT acquisition and analysis protocols for clinical care and research purposes, and recommends specific measures for diagnosis of osteoporosis, assigning fracture risk and monitoring osteoporosis treatment effectiveness, among patients with neurological impairment. A systematic literature search of MEDLINE, EMBASE©, CINAHL and PubMed for available pQCT studies assessing bone health was carried out from inception to August 8th, 2017. The search was limited to individuals with neurological impairment (spinal cord injury, stroke and multiple sclerosis) as these groups have rapid and severe regional declines in bone mass. Of 923 references, we identified 69 that met review inclusion criteria. The majority of studies (n = 60) used the Stratec XCT 2000/3000 pQCT scanners as reflected in our evaluation of acquisition and analysis protocols. Overall congruence with the ISCD Official Positions was poor. Only 11% (n = 6) studies met quality reporting criteria for image acquisition and 32% (n = 19) reported their data analysis in a format suitable for reproduction.

Therefore, based on current literature synthesis, ISCD position statements standards and the authors' expertise, we propose acquisition and analysis protocols at the radius, tibia and femur sites using Stratec XCT 2000/3000 pQCT scanners among patients with neurological impairment

for clinical and research purposes in order to drive practice change, develop normative datasets and complete future meta-analysis to inform fracture risk and treatment efficacy evaluation.

Key words: pQCT, image acquisition, neurological impairment, spinal cord injuries, diagnosis, systematic review, treatment

INTRODUCTION

Advances in medical imaging (i.e., quantitative computed tomography and magnetic resonance imaging) during the last three decades have: enabled more comprehensive *in vivo* analysis of bone macro- and micro-structure; increased our overall knowledge and understanding of bone anatomy and physiology; and, improved diagnostic determination of the presence or absence of disease (osteoporosis) [1,2]. Nevertheless, in the clinical realm, diagnostic determination of the presence of low bone mass (osteoporosis), and the associated risk of non-vertebral and vertebral fragility fractures continues to rely predominantly on dual-energy X-ray absorptiometry (DXA) measures of areal bone mineral density (aBMD) and associated risk prediction tools (e.g., FRAX®, CAROC) as the current clinical "gold standard" [3–6].

DXA is low cost, widely available, with simple usability - lower aBMD values are associated with a higher likelihood of fragility fracture, and a greater likelihood the patient will benefit from medical therapy [7,8]. Despite these appealing features, the reliability of aBMD can be compromised by inherent inaccuracies and ambiguities in DXA interpretation [9–11]. The aBMD assessments do not consider bone size and, subsequently, a larger bone may appear more dense than a smaller one [2]. Furthermore, aBMD is derived from the assumption that the region of interest contains only calcified hard tissue and homogeneous soft tissues [10]. Further, DXA is currently unable to provide reliable estimations of three-dimensional bone geometry and structure, that are necessary for the assessment of bone strength [12] and associated fracture risk [13–15]. These limitations often lead to spuriously elevated absolute aBMD values among patients with bone disorders, such as osteoarthritic spondylosis and/or diffuse idiopathic skeletal hyperostosis [16].

In contrast to DXA measurements of aBMD, peripheral quantitative computed tomography (pQCT) and high resolution pQCT (HRpQCT) allow measurement of volumetric BMD (vBMD) *independent of bone size*. These scanners conduct sequential scanning (translation – rotation motion) in acquisition mode and acquire single-slice (pQCT) or multi-slice (HRpQCT) cross-sectional images. Further, pQCT scanners offer the means to assess bone cross-sectional geometry, and to separate bone into its trabecular and cortical compartments [17]. However, due to the narrow diameter of the scanner gantry, they cannot be applied to vertebral or proximal femur sites. Nonetheless, pQCT does provide information on apparent structural traits from appendicular bones, similar to data provided by clinical QCT at the lumbar spine and proximal femur [18–20]. Furthermore, pQCT scanners do not require transfer of patients onto the scanner bed, which is particularly appealing among individuals with neurological impairments who require gait aids or a manual or power wheelchair to move about their home or community [21].

Notwithstanding the aforementioned limitations of DXA assessment, the discrepancies in DXA and pQCT distribution throughout the world [22], and the volume of pQCT studies [23], the current official positions of the International Society for Clinical Densitometry (ISCD) [4,6,24,25], does not recommend routine use of pQCT for diagnosis of osteoporosis, fracture risk prediction or monitoring of treatment effectiveness. This position is in part due to incompatibility of pQCT data with DXA derived T-scores, inconsistency in measurement sites, acquisition and analysis protocols, lack of normative studies, and specific treatment thresholds [4,23,24,26,27]. The following research questions were specified by ISCD (2007 ISCD Official Positions [4]) to determine the generalizability of pQCT modalities in clinical settings: “1) What are the technical

limitations of pQCT assessment for specific patient groups? ; 2) Which are the optimum anatomical sites to scan? ; and most importantly, 3) Which parameter(s) should be measured and for which intervention (diagnosis, fracture risk prediction, or treatment monitoring)". These knowledge gaps constitute barriers to advancement of pQCT practice and routine clinical implementation of pQCT technology.

It is well recognized that disuse related declines in bone mass (e.g., after sustaining a spinal cord injury, SCI) [28–33] are more rapid and severe than age or postmenopausal related bone deterioration [34,35]. Consequently, monitoring time intervals of changes in bone traits (e.g., size, shape, density, structure) as detected by peripheral scanners are shorter in duration, when compared to the general aging population. As a result, this impairment group represents a unique model for determination of the most appropriate pQCT measures based on their clinimetric properties for diagnosis, fracture risk prediction and monitoring of therapy. Finally, individuals with SCI tend to fracture at the distal femur and proximal tibia rather than the spine or proximal femur, so pQCT scans may be more clinically relevant [36].

Thus, due to the current lack of consensus derived recommendations/guidelines for clinicians/researchers regarding pQCT implementation, we conducted a systematic literature search. Based on synthesis of the literature identified and the authors' expertise, we evaluated the quality reporting of pQCT methods according to the ISCD Official Positions' and available evidence to recommend the most appropriate pQCT acquisition and analysis protocols, measures for diagnosis of osteoporosis, assigning fracture risk and monitoring the effectiveness of osteoporosis therapy among individuals with neurological impairment. Considering the

variety of pQCT-based studies, in-vivo human studies among individuals with neurological impairment, including SCI, stroke and multiple sclerosis (MS), were the focus of this review.

METHODS

Methodology

A systematic literature search for peer-reviewed articles was conducted in four databases MEDLINE (OVID interface), EMBASE©, CINAHL and PubMed. The search included all published reports from 1946 (MEDLINE and PubMed), 1947 (EMBASE©) and 1937 (CINAHL) until August 8th, 2017. The search strategy used the following terms to capture the key concepts: SCI, Stroke, Multiple Sclerosis, pQCT, HR-pQCT, long bones, bone loss and bone traits. The search strategy employed an algorithm for each term, which was refined for each database, maximizing the use of available filters and qualifiers in order to maximize manuscript capture and minimize inclusion of irrelevant records (Appendix 1).

A total of 923 references were identified; 156 (MEDLINE), 358 (EMBASE), 40 (CINAHL) and 369 (PubMed). However, the search failed to identify some articles [37–40] on related topics known to the authors; these articles were also included in the review process.

Selection process

The primary author (TC) eliminated duplicate records (n = 301). Following a first level review of the abstract title and body of the remaining studies, the primary author eliminated animal studies not excluded by the search strategy (n = 26), ex vivo studies (n = 13), and studies unrelated to the imaging modalities of interest (i.e., modalities that cannot be directly used for densitometric measurements) and/or to the desired sites of assessment including the radius, tibia or femur anatomic sites (n = 480).

Following a second level review of the method sections of all remaining studies (n = 103), the primary author excluded study protocols (n = 1), studies irrelevant to the populations of interest (n = 8) and modality of interest (n = 21), and review papers (n = 4). Of the remaining 69 studies, 67 used pQCT and 2 HRpQCT for bone health assessment. The article screening process is illustrated in Figure 1.

[PREFERRED LOCATION OF FIGURE 1]

Appraisal of evidence

The following data were abstracted from the selected manuscripts: (i) the material and methods sections were searched for references regarding study design (observational/ interventional, cross-sectional/ longitudinal), patient population, scanner type, reference lines used, imaging site(s) selection, voxel size, slice thickness, method used for data analysis; and, (ii) the results and discussion sections were hand searched for references regarding bone traits that showed significant changes over the study duration or significant between group differences ($p<0.05$) and their clinimetric properties (i.e. the precision and least significant change), or traits used for bone strength estimation and/or fracture risk prediction. These bone traits were then deemed meaningful for bone assessment by peripheral scanners and recorded. Traits that were reported as significant by at least 20% of studies (with similar study design), were recommended for inclusion in future minimum data sets (research and clinical), required to inform the development of normative datasets.

To guarantee study reproducibility and comparability, the 2015 ISCD Official Positions state that quality reporting of pQCT methods should specify details regarding the pQCT acquisition and analysis [4,24]. Specifically, all image acquisition protocols should include: scanner

make/model, bone length measurement methods; reference line selection, voxel size, and slice thickness settings; scanner translation speed, and specification of the imaging sites. Analysis protocols should clearly describe: the software version; analysis modes, and software thresholds used. The following sections describe the available abstracted data regarding pQCT scan acquisition parameters (anatomic site selection, reference line selection, voxel size, etc.), and scan analysis methods (i.e., used contour and peel modes, and specific thresholds) among individuals with SCI, Stroke and MS.

RESULTS

Imaging modalities

The majority of reviewed studies (n = 60) used single-slice scanners, either XCT 2000 or XCT 3000 (Stratec Medizintechnik GmbH, Pforzheim, Germany), with two exceptions, two studies which used the multi-slice XtremeCT (Scanco Medical AG, Bassersdorf, Switzerland) [41,42]. A few studies (n = 6) used predecessors of these scanners e.g., XCT 960, Densiscan 1000/2000 [29,32,38,43–45], and one study used the specially designed OsteoQuant© peripheral scanner [46] (Table 1).

[PREFERRED LOCATION OF TABLE 1]

As the search strategy identified only two HRpQCT-based studies [41,42], the evidence abstracted from these studies was considered insufficient for drawing specific conclusions, and therefore was omitted from further synthesis and the article recommendations. Further, the XCT 960 and Densiscan scanners are obsolete and are now sparsely available [Personal communication with Stratec Medizintechnik GmbH and Scanco Medical], and the OsteoQuant© scanner is a unique laboratory product. As newer clinical scanners (XCT 2000/3000 and XtremeCT I/II) are routinely

used for current clinical studies, the further description of these aforementioned outdated scanners was deemed irrelevant for the purpose of this manuscript; thus, no further discussion regarding the XtremeCT (n = 2), XCT 960 (n = 2), Densiscan (n = 4) and OsteoQuant© (n = 1) scanner is included. Of note, technical details of both XCT 2000 and 3000 scanners were abstracted from the manufacturers' websites and supplemental materials, and are presented in Table 2.

[PREFERRED LOCATION OF TABLE 2]

Image acquisition

Anatomic site selection

Of the sixty pQCT studies selected for inclusion in this review, 21 (35%) studies did not report the methodology used for determining bone length and identifying reference lines for each region of interest [37–39,47–65]; further, an additional 25 (42%) studies reported the distal endplate or joint gap as a reference line, without any specific details regarding how these were identified, or the reference lines assigned [28,63,66–88].

In the remaining fourteen studies (25%) [30,31,89–100], the radius bone length was measured from the humero-radial joint cleft to the medial aspect of the styloid process, the tibia bone length from the most distal palpable end of the medial malleolus to the most proximal edge of the medial tibial plateau (the medial joint cleft), and the femoral length was either approximated to be equal to tibial length as suggested by Eser et al. [93], or measured from the most proximal palpable limit of the greater trochanter, to the most distal limit of the lateral femoral condyle. For the radius and tibia, reference lines were placed at the flattest portion of the plateau of the tibial or radial endplate, respectively. For the proximal tibia imaging, the reference line was

placed on the proximal end of the more distal of the two condyles of the tibia (medial condyle of the tibia). For the femur, the reference line was placed at the distal limit of the lateral femoral condyle.

Imaging sites reported in the selected literature and the rationale for their inclusion is briefly outlined in Table 3. The majority of studies used the manufacturer's recommended imaging sites for trabecular bone assessment (4% of radius, tibia and femur length), cortical bone assessment (38% of tibia and 25% of femur length) and muscle assessment (66% of radius and tibia length, Table 4, Figure 2).

[PREFERRED LOCATION OF FIGURE 1]

Voxel size selection

Despite the importance of reporting voxel sizes [24] in pQCT study methods, 14/60 studies (23%) did not report this important detail [47,49,50,53,55,59,60,65,68–70,72,77,85]. From the remaining studies, the majority used either 0.4 x 0.4 mm (epiphysis) or 0.5 x 0.5 mm (diaphysis) voxel sizes for radial and tibial assessments, and a reduced 0.3 x 0.3 mm voxel sizes for femoral assessment due to a very thin cortical shell at the distal femur sites. The slice thickness varied between 2 – 2.5 mm (Table 4).

Of note, only 6 (10%) studies [30,31,89,93,94,99] met quality reporting criteria for image acquisition based on ISCD Official Positions.

[PREFERRED LOCATION OF TABLE 3 AND 4]

Scan Analysis

Twenty of the selected studies (33%) in this review, did not report details regarding image analysis [28,32,37–39,47,49–51,53,55,56,59,60,62,65,69,70,76,77]. Further, 21 (35%) studies provided incomplete

descriptions (Table 5). Nevertheless, based on the authors' knowledge of the Stratec analysis software, we were able to abstract or infer the following patterns for assessment of *epiphyseal sites*:

- For the periosteal border (total bone cross-section) detection, all available contour modes were used, with specific research groups selecting their own threshold levels; the following thresholds were used in an almost equal number of studies: 130, 150, 169, 180, and 200 mg/cm^3;
- The cortical compartments were not analyzed, with the exception of two studies [66,80], presumably due to the thin cortex in these locations and poor endosteal border detection of cortical bone [101,102];
- Approximately half of the studies used threshold driven selection of the trabecular compartment (Peel mode 2), mostly set to a threshold value of 400 mg/cm^3. The remaining studies appear to have used Peel mode 1 with trabecular compartment detection set to 45% of total bone area.

For *diaphyseal sites*, almost all research groups used similar analysis settings:

- For assessment of total bone cross-section, the vast majority of studies used unspecified contour mode (presumably mode 1) with the threshold set to 280 mg/cm^3;
- For assessment of cortical bone cross-section, the vast majority of studies used unspecified separation mode (presumably 1 or 2) with the threshold set to 710 mg/cm^3;
- If the stress strain index (SSI) analysis was reported separately (8 studies [31,48,54,68,72,93,94,103]), the most frequently used threshold was 280 mg/cm^3.

Of particular note, only 19 (32%) studies met quality reporting criteria for image analysis based on the ISCD Official Positions.

[PREFERRED LOCATION OF TABLE 5]

Reported bone traits with significant responses

The most frequently reported bone traits showing significant changes or between-group differences over all reviewed studies are summarized in Table 6. The precision and least significant changes for particular bone traits (Table 6) at each of the manufacturer's suggested imaging sites are shown in Table 7, which displays the mean values derived from data provided in the following studies [17,31,73,81,83,95,104–108].

[PREFERRED LOCATION OF TABLE 6 AND 7]

Observational studies: The most frequently reported bone traits showing significant changes in observational studies at epiphyseal sites of radius, tibia and femur were total bone mineral content (BMCto), total vBMD (BMDto) and trabecular vBMD (BMDt). At diaphyseal sites, traits demonstrating consistent clinically significant changes within the reviewed studies were BMCto, cortical BMC (BMCc), cortical cross-sectional area (CSAc) and cortical thickness (CoTh).

Interventional studies: Interventions featured either a form of exercise (e.g., functional electrical stimulation, partial body-weight supported treadmill training, robotic exoskeleton walking, standing or variety of weight-bearing activities to enhance lower extremities bone strength in stroke survivors) [37,39,40,45,47,51,55,57,62,65,71,72,78,86,89,91,92,109] or use of oral or intravenous bisphosphonate therapy [52,77].

Similar to observational studies, the traits that showed the largest responses to interventions were BMCto, trabecular BMC (BMCt) and BMDt, and BMCto, BMCc and CoTh at epiphyseal and diaphyseal sites of the radius, tibia and femur, respectively.

Bone strength and fracture discrimination: The bone strength traits often showing significant between group differences in the currently reviewed pQCT-based studies were the bone strength index (BSI) and stress-strain index (SSI) at epiphyseal and diaphyseal sites, respectively. The bone traits that were able to distinguish between individuals with, and without, a history of fracture were BMDt and polar moment of inertia (PMI).

DISCUSSION

Imaging modalities

All pQCT scanners selected for inclusion in this review, have distinct advantages and disadvantages, which limit their usability for particular patient groups, measurement sites, and purposes. The XCT peripheral scanners use the single-slice technology. In contrast to the multi-slice high-resolution technology scanners (HRpQCT), they do not acquire high resolution images, isotropic voxel sizes (the same voxel size in plane and axial direction) and full 3D imaging of the field of view. Nevertheless, these XCT scanners have the advantage of somewhat faster image acquisition times, and consequently a lower frequency of movement artifacts, lower radiation dose (x-ray beam is shaped according to detector size), and calibration prior to projection (the X-ray source and detector move off the field of view, while measurements of the empty field and the dark bias signal are performed).

The XCT 2000 is the lightest and the most portable of these scanners; it can be placed on a moving and height adjustable platform which makes it an ideal device for studies of individuals

with neurological impairment where restricted patient mobility necessitates greater scanner mobility. Operators or technologists can adjust the scanner position according to scan or patient specific needs [21]. This scanner can acquire images of the humerus, radius, distal femur and tibia. The reach is, however, limited by the maximal distance of travel (40 cm) and the gantry opening (14 cm). Due to these limitations in the gantry movement, the device does not allow measurements of the entire lower limb in adults. Thus, the patient has to be repositioned for scans of the distal femur and proximal tibia. In addition, the limited gantry opening restricts the use of this scanner to individuals with a smaller limb circumference. Consequently, this reduces the usability of this scanner for muscular or obese patients with a wide calf circumference, or measurement of more proximal femur sites.

The XCT 3000 scanner is larger and heavier than the XCT 2000, necessitating that it remain in place. However, it's larger gantry opening (30 cm), allows screening of the limbs with larger circumferences and more proximal sites of the femur. Bone traits yielded by both scanners have excellent agreement and are highly correlated; r = 0.90–0.99 for cortical vBMD (BMDc), with r = 0.97–0.99 for all other traits across measured sites [110,111]. Therefore, these scanners could be used interchangeably particularly during multi-centre clinical trials.

Image acquisition

The image acquisition time for one anatomical site (single-slice) for both pQCT scanners is ~ 90s (depending on limb diameter and scan speed). Short time periods for pQCT data acquisition reduces the appearance of movement artifacts in the resulting image. To avoid negative density values within images, Stratec pQCT scanners are calibrated so that fat tissue is equal to 0 and water ~55 mg/cm^3 of bone equivalent [112]

Anatomic site selection

The large variability in Stratec scanner settings allows users (researchers/clinicians/technologists) the potential to assess any bone location or region of interest provided that the desired region fits within the scanner gantry. This is especially beneficial when evaluating interventions where anatomically-localized intervention-specific responses are expected. However, the lack of standardized scanning protocols and the freedom to select a variety of anatomical sites restricts inter-study comparison [4] and limits our ability to establish recommendations for routine use of pQCT sites to measure vBMD in clinical practice, or to recommend minimal data elements for inclusion in research settings such as a clinical trial.

A recent study by Rittweger et al. [85], investigated the tibia of individuals with SCI (n = 9) by conducting a series of evenly distributed scans (in steps of 5% of the tibia length) and compared with results acquired from body height, weight and age matched able bodied individuals (n = 9). They found that bone (BMCto) is primarily lost at epiphyseal sites (the largest absolute bone lost being at proximal epiphysis), and the largest reduction (expansion) of periosteal (endosteal) circumference occurs between 30% and 40%, and between 65% and 75% of tibia length. These results suggest that the measurement sites with optimal prognostic capability for clinical practice may be located at these sites. Nevertheless, larger-scale studies are needed to confirm this assumption.

In addition to variability in the region of interest or anatomic site selection, there is variability in the methodology for determining bone length, and identifying reference lines, for each region of interest. This variability in procedures combines to produce additional sources of variability

in scan acquisition. Accurate and precise measurements of bone length and reference line selection are crucial. In the worst case scenario, as investigated by Shields at al. [99], the scan location error can be up to ±3 mm. This slice misplacement at the ultra-distal tibia (4% site) can account for mean BMDt differences up to 2.3% and 4.6% in able-bodied individuals and individuals with SCI, respectively [99]. Within the distal femur region of interest, the mean BMDt differences were 2.6% and 2.4% for able-bodied individuals and individuals with SCI, respectively [90].

In other studies, authors evaluated the influence of a misplaced slice in a follow-up scan [113,114]. Marjanovic et al. reported that slice misplacement at the ultra-distal radius by 1.2 mm can result in mean BMDt and BMDto differences 3.8% and 4.8%, respectively. Further, in a study by Sun et al., the authors conducted an exhaustive investigation of changes in total cross-sectional area and BMDt at the ultra-distal sites of the radius and tibia with changes of slice position up to ±1 mm in 0.1 mm steps. They reported that the cross-sectional area changes by ~20 mm^2 for each 0.5 mm slice misplacement in both the radius and tibia. Further, the BMDt, with the same misplacement, changes by 3.3% and 0.8% in the radius and tibia, respectively. In addition, in the radius, slice misplacement by 1 mm proximally (distally) leads to a ~31 mm^2 (40 mm^2) change in bone cross-section and 5.8% increase (2.6% decrease) in BMDt. They also investigated changes in the precision of BMDt measurement, and suggest that the follow-up location can be considered to be the same location as the baseline measurement, if the total bone cross-section (CSAto) remains within ±10 mm^2 and ±20 mm^2 at the radius and tibia, respectively. Thus, site selection and potential errors in slice placement may have a profound impact on the interpretation of the therapeutic effectiveness of interventions. Therefore, to yield clinically

reliable results, uncompromised by the aforementioned issues, it is essential to set rigorous protocols for measurement of bone length and slice assignment particularly for longitudinal evaluation, that do not deviate throughout the study. For Stratec operating software version 5.5 and up, use of an automatic procedure of reference line placement by matching the baseline scan scout view and follow-up measurements for longitudinal studies is recommended. Ideally, the same acquisition protocols should be used in all pQCT studies. Of note, in longitudinal evaluations, bone length measurement should not be repeated after the baseline measurement in adults with a mature skeleton, to avoid further measurement errors.

Voxel size selection

The main disadvantage of Stratec pQCT scanners is low image resolution. Spatial resolution of the scanner is determined by the size of the smallest possible feature that can be detected. Resolution is typically represented by a point spread function (PSF). The PSF describes the response of an imaging system to a small point object (e.g., small bead), with the spread of the point object in the image characterizing the PSF. However, voxel size is commonly used to indicate differences in spatial resolution between different imaging modalities, given that the voxel size is greater than the PSF, not equivalent to the PSF. While standard XCT scanners have adjustable voxel size in range 0.2 – 1.0 mm and fixed slice thickness in range of 2.0 – 2.5 mm, the XCT Research+ scanners can theoretically reach voxel sizes down to 0.1 mm, with a slice thickness of 0.5 mm. This setting improves scanner spatial resolution and decreases partial volume effects, however, at the cost of a higher noise level, due to a finite number of X-rays quanta produced by the X-ray source. With smaller voxel size – less X-ray quanta are detected to create an image. Therefore, longer imaging (exposure) time, or increased X-ray quanta

energy, both increasing radiation dose, are key considerations when optimizing image quality. Of note, reducing slice thickness by a factor 5, assuming the radiation dose remains unchanged, will increase the noise by a factor of $\sqrt{5}$ [115]. Obviously, increasing the radiation dose is not a desired option in any setting and longer exposure times increase the potential for movement artifacts. This is especially important during radius measurements where even a subtle movement can radically decrease the reliability [116] and measurements among patients with neurological impairment who may have spasticity, tremor, clonus or other involuntary movements difficult to inhibit for prolonged periods of time.

Nevertheless, reducing the slice thickness from 2.2 mm to 0.6 mm while reducing scanning speed (~increasing radiation dose) to keep the same noise level, did not improve accuracy of assessed bone traits in a cadaver study conducted by Lala and colleagues [117].

These voxel size settings (0.4 x 0.4 mm or 0.5 x 0.5 mm for assessment of the radius and tibia, and 0.3 x 0.3 mm for assessment of the femur allow sufficiently accurate determination of bone densities of both bone compartments [108,118] and detection of cortical bone thicker than 2.0 – 2.5 mm [101,119]. With voxel size reduced to 0.2 x 0.2 mm for epiphyseal sites; with use of a dedicated software, bone micro-architecture (bone volume fraction, trabecular number, trabecular separation and trabecular thickness) can be roughly estimated [73,74,117,120]. Nevertheless, these apparent micro-architecture traits differ substantially from traits obtained via high-resolution pQCT [117], and at this time there seems to be no additional diagnostic value, or clinical utility over standard pQCT-measured vBMD [121].

Data Analysis

Since introduction of the Stratec pQCT scanner, almost three decades ago, researchers have tried to determine the optimal means of analyzing the acquired images. The common approach is based on manufacturer-provided simple density threshold contour detection and peeling procedures [122,123]. This practice comes not only from its technical simplicity, but also from the need for reproducible results in clinical and research settings. However, these clinical needs are not always met by threshold based analyses [101,118,124,125], mainly due to partial volume effects, a relatively low signal to noise ratio, or the presence of movement artefacts.

Therefore, proper reporting of analysis modes and the threshold levels used, are the key reporting criteria to ensure reproducibility of future studies and assure inter-study comparability [24].

We found substantial variability in analysis parameters. It has been suggested that thresholds 169 mg/cm^3 and 130 mg/cm^3 are the optimal settings for assessment of able-bodied individuals [108,125] and individuals with SCI [21], respectively, yet a variety of thresholds are in use for periosteal border detection. However, the main discrepancy between studies stems from the selection of the peel mode. Dudley-Javoroski and Shields [90] found that the peel mode 1 (set to 45%) reduces mean BMDt by an average of 17.3% and 8% in comparison with threshold driven peel mode for subjects with SCI and able-bodied subjects, respectively. Further, for subjects with low BMDt, peel mode 1 yielded differences up to 30% from the value obtained with the threshold driven peel method. For subjects with higher density BMDt, differences between the two modes were smaller (~10%). Sievanen et al. [17] compared BMDt data obtained from both peel mode 1 and contour detection algorithm (peel mode 2, contour mode 2) and found large discrepancies (up to ±36 mg/cm^3) between the analysis methods. This data suggests results

from studies using different peel modes cannot be combined or directly compared. The peel mode 1 can be used in scenarios where investigators desire to compare similar bone regions between study cohorts, assuming that the trabecular deterioration occurs mainly in the center of the bone cross-section. This latter assumption, however, may not be true, as the trabecular bone adaptations to interventions vary across anatomical regions of the bone cross-section [71,92,126].

Although the threshold for cortical bone assessment was set to 710 mg/cm^3 (manufacturer's recommended value) in the majority of reviewed studies, it has been recognized that this threshold should be set to a lower value (~600-661 mg/cm^3) to correctly determine cortical bone geometry (e.g., CSAc) [101,108,118,124,125,127]. The manufacturer's recommended threshold also underestimates the BMDc value by ~10-15% [101] and a higher value (~1200 mg/cm^3) should be used to accurately determine BMDc [101,127]. Therefore, two distinct thresholds should be used to correctly assess CSAc and BMDc. The lower threshold value (661 mg/cm^3), however, provides BMDc values similar to those yielded by HRpQCT (mean error = -0.6%) [128], despite different density calibrations of the two modalities [112,129].

To date, two more sophisticated and reliable, threshold-free approaches have been developed to reduce dependence on threshold based analysis for pQCT data assessment, OsteoQ [130] and OBS [131,132]. Nevertheless, these methods are not routinely available for clinical use. The former is proprietary software developed by Gordon et al. and customers are charged an hourly rate for data analysis, and the latter was developed by Cervinka et al., available on request, for cortical bone detection at epiphyseal sites. In addition, the current evidence supporting their use in clinical studies is limited [126,133,134].

Reported bone traits with significant responses

Observational studies

Although only a limited number of reported bone traits showed clinically significant changes or important between group differences across the reviewed articles, these findings are not unexpected (Table 6). First, all of the reviewed studies used the manufacturer's threshold-based protocols that preclude accurate detection of cortical bone at epiphyseal sites [101,131]. Second, as the trabecular compartment accounts for the majority of bone cross-section at the epiphyseal site, all traits are likely to be directly affected by changes in trabecular structure. Third, at diaphyseal sites, where the bone is composed predominantly of thicker cortical bone, bone traits related to cortical bone cross-section or amount of bone mineral (BMCc), not density (BMDc), are the key parameters to monitor.

Obviously, one can speculate whether the assessment of BMDc at diaphyseal sites would provide any additional information as suggested by radial and polar BMDc assessment in young men [135] or postmenopausal athletes [136]. Nevertheless, to date, there is no evidence requiring bone anatomical sector analysis in individuals with neurological impairments and current evidence shows that BMDc only slightly decreases (2-4%) during the first 2-5 years post SCI or stroke [31,32,54,81], and recovers thereafter [31,54,95]. This decrease may be caused by intra-cortical remodeling (increased cortical porosity) as reported in HRpQCT-based study by Kazakia et al. [137] where cortical porosity was found to have the largest and most persistent response to 6 weeks of immobilization. Cortical porosity, however, cannot be detected by low resolution pQCT. Therefore, it seems that after sufficient cortical bone deterioration at the endocortical surface – bone adaptation to the new loading conditions, only reduced (more compact) cortical

bone cross-section is detected. Perhaps, including a total vBMD trait at diaphyseal sites in future studies may provide an explanation; if total bone cross-section remains stable, bone loss across the whole cross-section, would likely infer bone deterioration at the endocortical surface.

Interventional studies

In interventional studies, the observed changes have been presumed to be related to bone adaptation processes in the trabecular compartment and cortical bone cross-section at epiphyseal and diaphyseal sites, respectively. However, the mean numbers yielded from the whole bone cross-section may not provide the full picture, regarding the adaptation processes; specifically, in cortical and trabecular compartments or in anatomical directions. The actual benefit(s) resulted from a specific treatment may be lost in the analysis of the whole bone cross-section; whereas, anatomical sector analysis might improve sensitivity to longitudinal changes as reported by Dudley-Javoroski and Shields [71,92] and also suggested by Rantalainen et al. [138], Cervinka et al. [126] and Evans et al. [139] in able-bodied individuals. Consequently, treatments imposing a positive effect in a specific anatomical bone sector could result in a type two error (false negative results) based on whole cross-section assessment, although a simple regional or sector treatment modification may reveal positive effects on whole bone structure.

Bone strength and fracture risk prediction

The key role BSI and SSI traits play in estimation of long bone strength could be presumed as these traits reflect the strength of bone structure against compressive forces at the distal ends of long bones [140] and the torsional rigidity of the long bone shaft, respectively [124,141]. Nevertheless, only a limited number of studies presented thresholds for selected bone traits

(BMDt and PMI) intended to distinguish patients who are at high risk of fracture according to vBMD values [48,75,94].

In a retrospective study, Eser et al. [94] suggested using BMDt with thresholds set to 70 mg/cm^3 and 110 mg/cm^3 for distal tibia and femur, respectively. These thresholds were able to correctly determine, in one sample, 79% and 67% of patients with history of fracture in tibia and femur, respectively. Biggin et al. [48] evaluated distal tibia in pediatric patients and reported that patients did not sustain a fracture when their BMDt was higher than 100 mg/cm^3. However, a later study by Lala et al. [75] introduced data suggesting that this threshold may be placed even higher as patients with previous fracture(s) had mean (standard deviation - SD) BMDt equal to 84.4 (33.3) mg/cm^3. They also suggested that PMI was able to distinguish the patients with history of fracture from those without fracture. The mean PMI was equal to 32000 mm^4 and 47000 mm^4 in patients with fractures and without fractures, respectively, and the adjusted odds ratio (3.2) was significant (p = 0.038) [75].

Recommendations

The following recommendations stem from the described review, currently available data, and the authors' opinions/expertise.

Length measurement

Based on the abstracted evidence, we suggest that future studies should strictly measure bone length between following landmarks:

(i) the medial aspect of the styloid process and the humero-radial joint cleft for the radius;

(ii) the most distal palpable end of the medial malleolus and the most proximal edge of the medial tibial plateau (the medial join cleft) for the tibia; and,

(iii) the most distal limit of the lateral femoral condyle and the most proximal palpable limit of the greater trochanter.

Data acquisition – clinical studies

For measurement alignment, we suggest using the following reference lines (see Figure 2):

(i) the superior aspect of the cortical shell at the most distal and flattest portion of the plateau of the tibial or radial endplate;

(ii) the proximal end of the medial condyle of the tibia for proximal tibia imaging; and,

(iii) the distal limit of the lateral femoral condyle for imaging of femur.

To date, there are no available sensitivity studies, describing optimal imaging site/sites for assessment of bone responsiveness to interventions. Therefore, based on currently available knowledge, we propose that the following imaging sites be included in future clinical studies, as a part of minimum image acquisition protocol allowing interstudy comparability, should comprise:

(i) 4% and 66% for radius;

(ii) 4%, 38% and 66% for the tibia; and,

(iii) 4% and 25% for the femur.

In the event of interest in knee region imaging, imaging of the proximal tibia (96%) site may be used, keeping repeatability limits of this site in mind (Table 7).

Prior to completion of longitudinal analyses, clinicians and scientists should ensure that the CSAto in follow up scans does not differ by more than ±10 mm^2 (radius) and ±20 mm^2 (tibia) from the baseline scan, prior to conducting the analysis.

The 0.5 x 0.5 mm voxel size is sufficient for assessment of key bone traits (see Table 6) in radial, tibial and femoral diaphysis. A smaller voxel size of 0.4 x 0.4 mm should be used for assessment of the distal radius and tibia, and an even smaller voxel size 0.3 x 0.3 mm for measurements of femoral epiphysis as cortical bone is thinnest at this site.

The slice thickness, if applicable (all XCT Research+ scanners), should be selected within the range of 2 – 2.5 mm. The standard XCT scanners cannot reach thinner image slices (manufacturer pre-set slice thickness lies between 2 – 2.5mm) and therefore this range allows comparability between XCT scanners.

Data acquisition – clinical practice

In terms of screening patients for the presence or absence of osteoporosis, although their prognostic capability requires further validation, we recommend that the minimal image acquisition protocol should comprise the tibia 4%, 38% and 66% sites. The reference line should be placed at the superior aspect of the cortical shell at the most distal and flattest portion of the plateau of the tibial endplate (see Figure 2). The voxel size of 0.4 x 0.4 mm and 0.5 x 0.5 should be used for bone traits assessment in tibial epiphysis and diaphysis, respectively. The slice thickness should be selected within the range of 2 – 2.5 mm.

Summary of recommendations for pQCT image acquisition in clinical and research setting is appended in Table 8.

[PREFERRED LOCATION OF TABLE 8]

Data analysis selection

For bone detection at epiphyseal sites, locations mainly used for trabecular bone assessment, we recommend the use of contour mode 3 with thresholds set to 169 mg/cm^3 (able bodied subjects) and 130 mg/cm^3 (subjects with neurological impairment), and peel mode 2 set to 400 mg/cm^3. These settings will guarantee proper bone periosteal contour detection and clear separation of trabecular from subcortical bone, and assure comparability across studies.

At diaphyseal sites, we suggest the use of separation mode 4 with outer threshold set to 200 mg/cm^3 and inner threshold 650 mg/cm^3 to yield accurate cortical cross-sectional bone area.

Diagnosis

Clearly, large normative datasets are needed for diagnosis of osteoporosis based on Z-scores; a robust reference data set of this nature does not currently exist [4,24], partially due to the large variability in presented bone traits and measurement sites [23]. Therefore, based on the reviewed studies, we suggest reporting the following traits for radius, tibia and femur at the above suggested sites, as a future minimum data set to inform the development of normative datasets.

Epiphyseal sites:

- BMCto and BMDt

Diaphyseal sites:

- BMCto, BMCc, CSAc and CoTh

Although, BMDc, assessed at diaphyseal sites, was also reported as a trait consistently showing significant changes or between group differences in a large portion of reviewed studies (n = 21), we do not recommend use of this trait because of limitations provided in Discussion.

Monitoring therapies

For future longitudinal studies, we suggest monitoring the following bone traits that showed significant responses to intervention in reviewed studies.

Epiphyseal sites:

- BMCto and BMDt,

Diaphyseal sites:

- BMCto, BMCc and CoTh

Nevertheless, if feasible, future studies should also include anatomic regional analysis of cortical and trabecular compartments to improve sensitivity of bone assessment to longitudinal changes. Such a regional analysis is freely available as part of BoneJ for diaphyseal sites [(135)].

Bone strength and fracture risk prediction

Although some pQCT-based studies suggested use of a "hole" size in trabecular compartment [(130,142)] or cortical traits [(143)] as the optimal measures for fracture discrimination in the able-bodied population, the current review suggests that future pQCT-based studies should focus on establishing cut-off or threshold values to estimate risk of future fracture for BMDt and BSI, and PMI and SSI at epiphyseal and diaphyseal sites, respectively. Of note, based on current evidence [(75)], individuals with SCI with BMDt (measured at 4% site of tibia) above 120 mg/cm^3 are unlikely to sustain a fragility fracture.

Limitations

Some limitations warrant further discussion. When evaluating quality reporting of included studies, we used the recommendations imbedded in the 2015 ISCD Official Position Statement. However, there may be circumstances (e.g., word count restrictions imposed by journal editors)

in which authors reduce explicit details of their methodology (i.e., acquisition and data analysis protocols) by referring to their prior work or the standard methods used in their setting or laboratory. As source references were not considered in current review, these studies may have been evaluated as not fulfilling the quality reporting criteria because of the review criteria.

Further, the recommendations for land marking and measurement of bone length may be difficult or infeasible in some patients with neurological impairment due to body habitus, contracture, restricted range of motion, prior surgical intervention or fragility fracture in a region of interest, or changes in bone shape due to absence of muscle contraction or inability to weight bear.

Furthermore, prior to generalizing the aforementioned recommendations, there are several issues that require further consideration**.** First, despite efforts to identify all available literature concerning pQCT imaging used among populations with neurological impairment, the number of identified studies was relatively low, leaving the potential for biased evaluation of image acquisition and analysis protocols as well as bone traits that showed consistently significant changes or between group differences over all reviewed studies. Second, although all studies including SCI, stroke and MS populations were used for the abstraction of pQCT image acquisition and analysis protocols, the majority of evidence appraisal discussing issues relate to improper setting of these protocols are based on data derived from the SCI population; predominantly, from published literature regarding men with motor complete paraplegia. Therefore, following recommendations concerning image acquisition and analysis protocols may only be valid for this population. Nevertheless, we believe, the same standards can also be employed among individuals with other forms of neurological impairment such as MS, Stroke,

Parkinson's disease, Spina Bifida or Cerebral Palsy. The authors trust that data to validate, refine or revise our recommendations from others in the field, will follow publication of the enclosed recommendations.

CONCLUSIONS

The lack of consensus regarding scan acquisition and analysis protocols has been recognized by many authors [4,17,23,24,144] and remains a primary barrier to routine clinical implementation of pQCT technology. However, to our knowledge, no study evaluated what would be the most appropriate anatomic site and outcomes for determining the diagnosis of osteoporosis, predicting regional fracture, and monitoring of therapy efficacy/effectiveness for patients with neurological impairment. This lack of consensus limits implementation; creation of a robust age, sex, race and body size specific reference database is required to advance pQCT practice [23,24,26]. Despite the small number of selected studies for review inclusion, and the potential for biased recommendations, we have proposed minimum standard acquisition protocols, for use in both clinical practice and research settings, and analysis protocols for pQCT scanners among patients with neurological impairment for specific clinical indications including diagnosis of low bone mass, assigning fracture risk and determining therapy effectiveness. We anticipate that adherence to these recommendations would substantially advance the field and allow for future data synthesis (meta-analysis).

APPENDIX 1: Search strategies

MEDLINE search strategy

((exp Spinal Cord Injuries OR exp Paraplegia OR exp Quadriplegia OR hemiplegia OR exp paresis OR Spinal Cord Compresion OR (spinal cord injur* OR SCI).tw,kw OR (spinal cord adj3 (contusion* OR

trauma* OR transection* OR laceration* OR compression*)).tw,kw OR (paraplegia* OR quadriplegia* OR quadriparesis OR locked-in syndrome OR tetraplegia* OR hemiplegia* OR hemiparesis OR paresis).tw,kw OR exp Multiple Sclerosis OR exp Stroke OR (multiple sclerosis OR stroke*).tw,kw OR (cerebrovascular adj3 (accident* OR apoplexy)).tw,kw) AND (exp Tomography, X-Ray Computed OR peripheral quantitative computed tomography.tw,kw OR (peripheral adj2 computed tomography).tw,kw OR (pQCT* or HR-pQCT*).tw,kw) AND (radius OR femur OR tibia OR Bone Density OR ((bone* OR radius OR tibia* OR femur*) adj3 (health* OR quality OR density OR loss OR morphology OR strength OR recovery OR disease* OR status OR adapt* OR respon* OR geometr* OR structur* OR properties)).tw,kw OR (long adj2 bone*).af NOT (animals NOT (humans AND animals)).sh) limit to English language

EMBASE© search strategy

(exp Spinal Cord Injury OR Paraplegia OR Quadriplegia OR hemiplegia OR paresis OR (spinal cord injur* or SCI).tw,kw OR (spinal cord sdj3 contusion* OR trauma* OR transection* OR laceration* OR compression*)).tw,kw OR (paraplegia* OR quadriplegia* OR quadriparesis OR locked-in syndrome OR tetraplegia* OR hemiplegia* OR hemiparesis OR paresis).tw,kw OR exp Multiple Sclerosis OR exp cerebrovascular accident OR (multiple sclerosis OR stroke*).tw,kw OR (cerebrovascular adj3 (accident* OR apoplexy)).tw,kw) AND (exp computer assisted tomography OR peripheral quantitative computed tomography.tw,kw OR (peripheral adj2 computed tomography).tw,kw OR (pQCT* or HR-pQCT*).tw,kw) AND (exp long bone OR radius OR femur OR tibia OR Bone Density OR ((bone* OR radius OR tibia* OR femur*) adj3 (health* OR quality OR density OR loss OR morphology OR strength OR recovery OR disease* OR status OR adapt* OR respon* OR geometr* OR structur* OR properties)).tw,kw OR (long adj2 bone*).af NOT (animals NOT (humans AND animals)).sh) NOT (Conference Review.pt OR Conference Abstract.pt OR Short Survey.pt OR editorial.pt OR letter.pt OR note.pt) limit to English language

CINAHL search strategy

((MH “Spinal Cord Injuries+”) OR (MH “Paraplegia+”) OR (MH “Quadriplegia”) OR (MH “Hemiplegia”) OR (MH “Spinal Cord Compression”) OR TI (spinal cord injur* OR SCI) OR AB (spinal cord injur* OR SCI) OR TI (spinal cord N3 (contusion* OR trauma* OR transection* OR laceration* OR compression*)) OR AB (spinal cord N3 (contusion* OR trauma* OR transection* OR laceration* OR compression*)) OR TI (paraplegia* OR quadriplegia* OR quadriparesis OR locked-in syndrome OR tetraplegia* OR hemiplegia* OR hemiparesis OR paresis) OR AB (paraplegia* OR quadriplegia* OR quadriparesis OR locked-in syndrome OR tetraplegia* OR hemiplegia* OR hemiparesis OR paresis) OR (MH “Multiple Sclerosis”) OR (MH “Stroke+”) OR (TI (multiple sclerosis OR stroke*) OR AB (multiple sclerosis OR stroke*)) OR (TI (cerebrovascular N3 (accident* OR apoplexy)) OR AB (cerebrovascular N3 (accident* OR apoplexy)))) AND ((MH “Tomography, X-Ray Computed+”) OR (TI peripheral quantitative computed tomography OR AB peripheral quantitative computed tomography) OR (TI (peripheral N2 computed tomography) OR AB (peripheral N2 computed tomography)) OR (TI (pQCT* OR HR-pQCT*) OR AB (pQCT* OR HR-pQCT*)))

AND ((MH “Radius”) OR (MH “Femur+”) OR (MH “Tibia”) OR (MH “Bone Density”) OR (TI ((bone* OR radius OR tibia* OR femur*) N3 (health* OR quality OR density OR loss OR morphology OR strength OR recovery OR disease* OR status OR adapt* OR respon* OR geometr* OR structur* OR properties)) OR AB ((bone* OR radius OR tibia* OR femur*) N3 (health* OR quality OR density OR loss OR morphology OR strength OR recovery OR disease* OR status OR adapt* OR respon* OR geometr* OR structur* OR properties)) OR TX (long N2 bone*))

PubMed search strategy

(spinal cord injury [MeSH Terms] OR paraplegia [MeSH Terms] OR quadriplegia [MeSH Terms] OR paresis [MeSH Terms] OR spinal cord compression [MeSH Terms] OR (spinal cord injur* [Title/Abstract] OR SCI [Title/Abstract]) OR (spinal cord [Title/Abstract] AND (contusion* [Title/Abstract] OR trauma* [Title/Abstract] OR transection* [Title/Abstract] OR laceration* [Title/Abstract] OR compression* [Title/Abstract])) OR (paraplegia* [Title/Abstract] OR quadriplegia* [Title/Abstract] OR quadriparesis [Title/Abstract] OR locked-in syndrome [Title/Abstract] OR tetraplegia* [Title/Abstract] OR hemiplegia* [Title/Abstract] OR hemiparesis [Title/Abstract] OR paresis [Title/Abstract]) OR multiple sclerosis [MeSH Terms] OR stroke [MeSH Terms] OR (multiple sclerosis [Title/Abstract] OR stroke* [Title/Abstract]) OR (cerebrovascular [Title/Abstract] AND (accident* [Title/Abstract] OR apoplexy [Title/Abstract]))) AND (Tomography, X-Ray Computed [MeSH Terms] OR peripheral quantitative computed tomography [Title/Abstract] OR (peripheral [Title/Abstract] AND computed tomography [Title/Abstract]) OR (pQCT* [Title/Abstract] OR HR-pQCT*[Title/Abstract])) AND (radius [MeSH Terms] OR femur [MeSH Terms] OR tibia [MeSH Terms] OR bone density [MeSH Terms] OR ((bone* [Title/Abstract] OR radius* [Title/Abstract] OR tibia* [Title/Abstract] OR femur* [Title/Abstract]) AND (health* [Title/Abstract] OR quality [Title/Abstract] OR density [Title/Abstract] OR loss [Title/Abstract] OR morphology [Title/Abstract] OR strength [Title/Abstract] OR recovery [Title/Abstract] OR disease* [Title/Abstract] OR status [Title/Abstract] OR adapt* [Title/Abstract] OR respon* [Title/Abstract] OR geometr* [Title/Abstract] OR struct* [Title/Abstract] OR properties [Title/Abstract])) OR long bone* [Title/Abstract]) AND (humans [MeSH Terms] AND English [Lang])

REFERENCES

1. Ito M. 2011 Recent progress in bone imaging for osteoporosis research. J Bone Miner Metab. *29*:131–140.
2. Griffith JF, Genant HK. 2012 New advances in imaging osteoporosis and its complications. Endocrine. *42*:39–51.
3. Kanis JA, Borgstrom F, De Laet C, *et al.* 2005 Assessment of fracture risk. Osteoporos Int. *16*:581–589.
4. Engelke K, Adams JE, Armbrecht G, *et al.* 2008 Clinical use of quantitative computed tomography and peripheral quantitative computed tomography in the management of osteoporosis in adults: the 2007 ISCD Official Positions. J Clin Densitom. *11*:123–162.
5. Kanis JA, McCloskey EV, Harvey NC, Johansson H, Leslie WD. 2015 Intervention Thresholds and the Diagnosis of Osteoporosis. J Bone Miner Res. *30*:1747–1753.
6. Shepherd JA, Schousboe JT, Broy SB, Engelke K, Leslie WD. 2015 Executive Summary of the 2015 ISCD Position Development Conference on Advanced Measures From DXA and QCT: Fracture Prediction Beyond BMD. J Clin Densitom. *18*:274–286.
7. Black DM, Thompson DE, Bauer DC, *et al.* 2000 Fracture risk reduction with alendronate in women with osteoporosis: the Fracture Intervention Trial. FIT Research Group. J Clin Endocrinol Metab. *85*:4118–4124.
8. Kanis JA, Johnell O, Black DM, *et al.* 2003 Effect of raloxifene on the risk of new vertebral fracture in postmenopausal women with osteopenia or osteoporosis: a reanalysis of the Multiple Outcomes of Raloxifene Evaluation trial. Bone. *33*:293–300.

9. Sievänen H. 2000 A physical model for dual-energy X-ray absorptiometry--derived bone mineral density. Invest Radiol. *35*:325–330.

10. Bolotin HH, Sievänen H. 2001 Inaccuracies inherent in dual-energy X-ray absorptiometry in vivo bone mineral density can seriously mislead diagnostic/prognostic interpretations of patient-specific bone fragility. J Bone Miner Res. *16*:799–805.

11. Bolotin HH. 2004 The significant effects of bone structure on inherent patient-specific DXA in vivo bone mineral density measurement inaccuracies. Med Phys. *31*:774–788.

12. Sievänen H. 2010 Bone densitometry and true BMD accuracy for predicting fractures: what are the alternatives? Int J Clin Rheumatol. *5*:371–385.

13. Broy SB, Cauley JA, Lewiecki ME, Schousboe JT, Shepherd JA, Leslie WD. 2015 Fracture Risk Prediction by Non-BMD DXA Measures: the 2015 ISCD Official Positions Part 1: Hip Geometry. J Clin Densitom. *18*:287–308.

14. Delmas PD, Seeman E. 2004 Changes in bone mineral density explain little of the reduction in vertebral or nonvertebral fracture risk with anti-resorptive therapy. Bone. *34*:599–604.

15. Li Z, Chines AA, Meredith MP. 2004 Statistical validation of surrogate endpoints: is bone density a valid surrogate for fracture? J Musculoskelet Neuronal Interact. *4*:64–74.

16. Gregson CL, Hardcastle SA, Cooper C, Tobias JH. 2013 Friend or foe: high bone mineral density on routine bone density scanning, a review of causes and management. Rheumatol Oxf Engl. *52*:968–985.

17. Sievänen H, Koskue V, Rauhio A, Kannus P, Heinonen A, Vuori I. 1998 Peripheral quantitative computed tomography in human long bones: evaluation of in vitro and in vivo precision. J Bone Miner Res. *13*:871–882.

18. Lang TF. 2010 Quantitative computed tomography. Radiol Clin North Am. *48*:589–600.

19. Melton LJ 3rd, Riggs BL, Keaveny TM, *et al.* 2007 Structural determinants of vertebral fracture risk. J Bone Miner Res. *22*:1885–1892.

20. Melton LJ 3rd, Riggs BL, Keaveny TM, *et al.* 2010 Relation of vertebral deformities to bone density, structure, and strength. J Bone Miner Res. *25*:1922–1930.

21. Giangregorio LM, Gibbs JC, Craven BC. 2016 Measuring muscle and bone in individuals with neurologic impairment; lessons learned about participant selection and pQCT scan acquisition and analysis. Osteoporos Int. *27*:2433–2446.

22. Adams J. 2015 Quantitative computed tomography in children and adolescents. RAD Mag. *41*:33–35.

23. Fonseca A, Gordon CL, Barr RD. 2013 Peripheral quantitative computed tomography (pQCT) to assess bone health in children, adolescents, and young adults: a review of normative data. J Pediatr Hematol Oncol. *35*:581–589.

24. Adams JE, Engelke K, Zemel BS, Ward KA, International Society of Clinical Densitometry. 2014 Quantitative computer tomography in children and adolescents: the 2013 ISCD Pediatric Official Positions. J Clin Densitom. *17*:258–274.

25. Zysset P, Qin L, Lang T, *et al.* 2015 Clinical Use of Quantitative Computed Tomography-Based Finite Element Analysis of the Hip and Spine in the Management of Osteoporosis in Adults: the 2015 ISCD Official Positions-Part II. J Clin Densitom. *18*:359–392.

26. MacIntyre NJ, Lorbergs AL. 2012 Imaging-Based Methods for Non-invasive Assessment of Bone Properties Influenced by Mechanical Loading. Physiother Can. *64*:202–215.

27. Panisset MG, Galea MP, El-Ansary D. 2016 Does early exercise attenuate muscle atrophy or bone loss after spinal cord injury? Spinal Cord. *54*:84–92.

28. Coupaud S, McLean AN, Allan DB. 2009 Role of peripheral quantitative computed tomography in identifying disuse osteoporosis in paraplegia. Skeletal Radiol. *38*:989–995.

29. de Bruin ED, Dietz V, Dambacher MA, Stüssi E. 2000 Longitudinal changes in bone in men with spinal cord injury. Clin Rehabil. *14*:145–152.

30. Dudley-Javoroski S, Shields RK. 2012 Regional cortical and trabecular bone loss after spinal cord injury. J Rehabil Res Dev. *49*:1365–1376.

31. Eser P, Frotzler A, Zehnder Y, *et al.* 2004 Relationship between the duration of paralysis and bone structure: a pQCT study of spinal cord injured individuals. Bone. *34*:869–880.

32. Lazoura O, Groumas N, Antoniadou E, *et al.* 2008 Bone Mineral Density Alterations in Upper and Lower Extremities 12 Months After Stroke Measured by Peripheral Quantitative Computed Tomography and DXA. J Clin Densitom. *11*:511–517.

33. Sievänen H. 2010 Immobilization and bone structure in humans. Arch Biochem Biophys. *503*:146–152.

34. Hangartner T. 1995 Osteoporosis Due to Disuse. Phys Med Rehabil. *6*:579–594.

35. Takata S, Yasui N. 2001 Disuse osteoporosis. J Med Investig JMI. *48*:147–156.

36. Craven BC, Verrier M, Balioussis C, *et al.* 2012 Rehabilitation Environmental e-Scan Atlas: Capturing Capacity in Canadian SCI Rehabilitation C Y Lee, J Prescott, S Modder, and C Andrews, eds. . Rick Hansen Institute. Available at: http://rickhanseninstitute.org/images/stories/ESCAN/RHESCANATLAS2012WEB_2014.pdf.

37. Dudley-Javoroski S, Shields RK. 2008 Dose estimation and surveillance of mechanical loading interventions for bone loss after spinal cord injury. Phys Ther. *88*:387–396.

38. Fezoulidis NI, Tassiopoulos N, Papadaki PJ, *et al.* 2009 77 A pQCT Study of the Forearm in Multiple Sclerosis Patients. J Clin Densitom. *12*:122–123.

39. Kakebeeke TH, Hofer PJ, Frotzler A, Lechner HE, Hunt KJ, Perret C. 2008 Training and detraining of a tetraplegic subject: high-volume FES cycle training. Am J Phys Med Rehabil. *87*:56–64.

40. Pang MYC, Lau RWK. 2010 The effects of treadmill exercise training on hip bone density and tibial bone geometry in stroke survivors: a pilot study. Neurorehabil Neural Repair. *24*:368–376.

41. Wuermser L-A, Beck LA, Lamb JL, Atkinson EJ, Amin S. 2015 The effect of low-magnitude whole body vibration on bone density and microstructure in men and women with chronic motor complete paraplegia. J Spinal Cord Med. *38*:178–186.

42. Gibbons RS, Beaupre GS, Kazakia GJ. 2016 FES-rowing attenuates bone loss following spinal cord injury as assessed by HR-pQCT. Spinal Cord Ser Cases. *2*:15041.

43. de Bruin ED, Vanwanseele B, Dambacher MA, Dietz V, Stüssi E. 2005 Long-term changes in the tibia and radius bone mineral density following spinal cord injury. Spinal Cord. *43*:96–101.

44. Frey-Rindova P, de Bruin ED, Stüssi E, Dambacher MA, Dietz V. 2000 Bone mineral density in upper and lower extremities during 12 months after spinal cord injury measured by peripheral quantitative computed tomography. Spinal Cord. *38*:26–32.

45. de Bruin ED, Frey-Rindova P, Herzog RE, Dietz V, Dambacher MA, Stüssi E. 1999 Changes of tibia bone properties after spinal cord injury: effects of early intervention. Arch Phys Med Rehabil. *80*:214–220.

46. Hangartner TN, Rodgers MM, Glaser RM, Barre PS. 1994 Tibial bone density loss in spinal cord injured patients: Effects of FES exercise. J Rehabil Res Dev. *31*:50–61.

47. Ashe MC, Eng JJ, Krassioukov AV, Warburton DER, Hung C, Tawashy A. 2010 Response to functional electrical stimulation cycling in women with spinal cord injuries using dual-energy X-ray absorptiometry and peripheral quantitative computed tomography: a case series. J Spinal Cord Med. *33*:68–72.

48. Biggin A, Briody JN, Ramjan KA, Middleton A, Waugh M-CA, Munns CF. 2013 Evaluation of bone mineral density and morphology using pQCT in children after spinal cord injury. Dev Neurorehabilitation. *16*:391–397.

49. Dionyssiotis Y, Trovas G, Galanos A, *et al.* 2007 Bone loss and mechanical properties of tibia in spinal cord injured men. J Musculoskelet Neuronal Interact. *7*:62–68.

50. Dionyssiotis Y, Stathopoulos K, Trovas G, Papaioannou N, Skarantavos G, Papagelopoulos P. 2015 Impact on bone and muscle area after spinal cord injury. BoneKEy Rep. *4*:633.

51. Dudley-Javoroski S, Petrie MA, McHenry CL, Amelon RE, Saha PK, Shields RK. 2016 Bone architecture adaptations after spinal cord injury: impact of long-term vibration of a constrained lower limb. Osteoporos Int. *27*:1149–1160.

52. Dudley-Javoroski S, Amelon R, Liu Y, Saha PK, Shields RK. 2014 High bone density masks architectural deficiencies in an individual with spinal cord injury. J Spinal Cord Med. *37*:349–354.

53. Eser P, Schiessl H, Willnecker J. 2004 Bone loss and steady state after spinal cord injury: a cross-sectional study using pQCT. J Musculoskelet Neuronal Interact. *4*:197–198.

54. Frotzler A, Berger M, Knecht H, Eser P. 2008 Bone steady-state is established at reduced bone strength after spinal cord injury: A longitudinal study using peripheral quantitative computed tomography (pQCT). Bone. *43*:549–555.

55. Frotzler A, Coupaud S, Perret C, Kakebeeke TH, Hunt KJ, Eser P. 2009 Effect of detraining on bone and muscle tissue in subjects with chronic spinal cord injury after a period of electrically-stimulated cycling: a small cohort study. J Rehabil Med. *41*:282–285.

56. Gislason MK, Coupaud S, Sasagawa K, *et al.* 2014 Prediction of risk of fracture in the tibia due to altered bone mineral density distribution resulting from disuse: a finite element study. Proc Inst Mech Eng. *228*:165–174.

57. Golomb MR, McDonald BC, Warden SJ, *et al.* 2010 In-Home Virtual Reality Videogame Telerehabilitation in Adolescents With Hemiplegic Cerebral Palsy. Arch Phys Med Rehabil. *91*:1–8.

58. Rittweger J, Gerrits K, Altenburg T, Reeves N, Maganaris CN, de Haan A. 2006 Bone adaptation to altered loading after spinal cord injury: a study of bone and muscle strength. J Musculoskelet Neuronal Interact. *6*:269–276.

59. Sherk KA, Sherk VD, Anderson MA, Bemben DA, Bemben MG. 2013 Differences in Tibia Morphology Between the Sound and Affected Sides in Ankle-Foot Orthosis-Using Survivors of Stroke. Arch Phys Med Rehabil. *94*:510–515.

60. Totosy de Zepetnek JO, Craven BC, Giangregorio LM. 2012 An evaluation of the muscle-bone unit theory among individuals with chronic spinal cord injury. Spinal Cord. *50*:147–152.

61. Varzi D, Coupaud SAF, Purcell M, Allan DB, Gregory JS, Barr RJ. 2015 Bone morphology of the femur and tibia captured by statistical shape modelling predicts rapid bone loss in acute spinal cord injury patients. Bone. *81*:495–501.

62. Gibbons RS, McCarthy ID, Gall A, Stock CG, Shippen J, Andrews BJ. 2014 Can FES-rowing mediate bone mineral density in SCI: A pilot study. Spinal Cord. 52:S4–S5.

63. Coupaud S, Gislason MK, Purcell M, Sasagawa K, Tanner KE. 2017 Patient-specific bone mineral density distribution in the tibia of individuals with chronic spinal cord injury, derived from multi-slice peripheral Quantitative Computed Tomography (pQCT) - A cross-sectional study. Bone. *97*:29–37.

64. Gibbs JC, Brown ZM, Wong AKO, Craven BC, Adachi JD, Giangregorio LM. 2017 Measuring Marrow Density and Area Using Peripheral Quantitative Computed Tomography at the Tibia: Precision in Young and Older Adults and Individuals With Spinal Cord Injury. J Clin Densitom. *25*.

65. Karelis AD, Carvalho LP, Castillo MJ, Gagnon DH, Aubertin-Leheudre M. 2017 Effect on body composition and bone mineral density of walking with a robotic exoskeleton in adults with chronic spinal cord injury. J Rehabil Med. *49*:84–87.

66. Ashe MC, Fehling P, Eng JJ, Khan KM, McKay HA. 2006 Bone geometric response to chronic disuse following stroke: a pQCT study. J Musculoskelet Neuronal Interact. *6*:226–233.

67. Coupaud S, McLean AN, Lloyd S, Allan DB. 2012 Predicting patient-specific rates of bone loss at fracture-prone sites after spinal cord injury. Disabil Rehabil. *34*:2242–2250.

68. Coupaud S, McLean AN, Purcell M, Fraser MH, Allan DB. 2015 Decreases in bone mineral density at cortical and trabecular sites in the tibia and femur during the first year of spinal cord injury. Bone. *74*:69–75.

69. Dionyssiotis Y, Lyritis GP, Papaioannou N, Papagelopoulos P, Thomaides T. 2009 Influence of neurological level of injury in bones, muscles, and fat in paraplegia. J Rehabil Res Dev. *46*:1037–1044.

70. Dionyssiotis Y, Lyritis GP, Mavrogenis AF, Papagelopoulos PJ. 2011 Factors influencing bone loss in paraplegia. Hippokratia. *15*:54–59.

71. Dudley-Javoroski S, Shields RK. 2008 Asymmetric bone adaptations to soleus mechanical loading after spinal cord injury. J Musculoskelet Neuronal Interact. *8*:227–238.

72. Frotzler A, Coupaud S, Perret C, *et al.* 2008 High-volume FES-cycling partially reverses bone loss in people with chronic spinal cord injury. Bone. *43*:169–176.

73. Giangregorio L, Lala D, Hummel K, Gordon C, Craven BC. 2013 Measuring Apparent Trabecular Density and Bone Structure Using Peripheral Quantitative Computed Tomography at the Tibia: Precision in Participants With and Without Spinal Cord Injury. J Clin Densitom. *16*:139–146.

74. Gibbs JC, Craven BC, Moore C, Thabane L, Adachi JD, Giangregorio LM. 2015 Muscle Density and Bone Quality of the Distal Lower Extremity Among Individuals with Chronic Spinal Cord Injury. Top Spinal Cord Inj Rehabil. *21*:282–293.

75. Lala D, Craven BC, Thabane L, *et al.* 2014 Exploring the determinants of fracture risk among individuals with spinal cord injury. Osteoporos Int. *25*:177–185.

76. McCarthy ID, Bloomer Z, Gall A, Keen R, Ferguson-Pell M. 2012 Changes in the structural and material properties of the tibia in patients with spinal cord injury. Spinal Cord. *50*:333–337.

77. Ooi HL, Briody J, McQuade M, Munns CF. 2012 Zoledronic acid improves bone mineral density in pediatric spinal cord injury. J Bone Miner Res. *27*:1536–1540.

78. Pang MYC, Ashe MC, Eng JJ, McKay HA, Dawson AS. 2006 A 19-week exercise program for people with chronic stroke enhances bone geometry at the tibia: a peripheral quantitative computed tomography study. Osteoporos Int. *17*:1615–1625.

79. Pang MYC, Ashe MC, Eng JJ. 2008 Tibial bone geometry in chronic stroke patients: influence of sex, cardiovascular health, and muscle mass. J Bone Miner Res. *23*:1023–1030.

80. Pang MYC, Ashe MC, Eng JJ. 2010 Compromised bone strength index in the hemiparetic distal tibia epiphysis among chronic stroke patients: the association with cardiovascular function, muscle atrophy, mobility, and spasticity. Osteoporos Int. *21*:997–1007.

81. Pang MYC, Yang FZH, Lau RWK, Cheng AQ, Li LSW, Zhang M. 2012 Changes in bone density and geometry of the upper extremities after stroke: a case report. Physiother Can. *64*:88–97.

82. Pang MYC, Cheng AQ, Warburton DE, Jones AYM. 2012 Relative impact of neuromuscular and cardiovascular factors on bone strength index of the hemiparetic distal radius epiphysis among individuals with chronic stroke. Osteoporos Int. *23*:2369–2379.

83. Pang MYC, Zhang M, Li LSW, Jones AYM. 2013 Changes in bone density and geometry of the radius in chronic stroke and related factors: a one-year prospective study. J Musculoskelet Neuronal Interact. *13*:77–88.

84. Pang MYC, Yang FZH, Jones AYM. 2013 Vascular elasticity and grip strength are associated with bone health of the hemiparetic radius in people with chronic stroke: implications for rehabilitation. Phys Ther. *93*:774–785.

85. Rittweger J, Goosey-Tolfrey VL, Cointry G, Ferretti JL. 2010 Structural analysis of the human tibia in men with spinal cord injury by tomographic (pQCT) serial scans. Bone. *47*:511–518.

86. Shields RK, Dudley-Javoroski S. 2006 Musculoskeletal plasticity after acute spinal cord injury: effects of long-term neuromuscular electrical stimulation training. J Neurophysiol. *95*:2380–2390.

87. Yang FZH, Pang MYC. 2015 Influence of chronic stroke impairments on bone strength index of the tibial distal epiphysis and diaphysis. Osteoporos Int. *26*:469–480.

88. Ireland A, Capozza RF, Cointry GR, Nocciolino L, Ferretti JL, Rittweger J. 2017 Meagre effects of disuse on the human fibula are not explained by bone size or geometry. Osteoporos Int. *28*:633–641.

89. Coupaud S, Jack LP, Hunt KJ, Allan DB. 2009 Muscle and bone adaptations after treadmill training in incomplete Spinal Cord Injury: a case study using peripheral Quantitative Computed Tomography. J Musculoskelet Neuronal Interact. *9*:288–297.

90. Dudley-Javoroski S, Shields RK. 2010 Longitudinal changes in femur bone mineral density after spinal cord injury: effects of slice placement and peel method. Osteoporos Int. *21*:985–995.

91. Dudley-Javoroski S, Saha PK, Liang G, Li C, Gao Z, Shields RK. 2012 High dose compressive loads attenuate bone mineral loss in humans with spinal cord injury. Osteoporos Int. *23*:2335–2346.

92. Dudley-Javoroski S, Shields RK. 2013 Active-resisted stance modulates regional bone mineral density in humans with spinal cord injury. J Spinal Cord Med. *36*:191–199.

93. Eser P, Frotzler A, Zehnder Y, Schiessl H, Denoth J. 2005 Assessment of anthropometric, systemic, and lifestyle factors influencing bone status in the legs of spinal cord injured individuals. Osteoporos Int. *16*:26–34.

94. Eser P, Frotzler A, Zehnder Y, Denoth J. 2005 Fracture threshold in the femur and tibia of people with spinal cord injury as determined by peripheral quantitative computed tomography. Arch Phys Med Rehabil. *86*:498–504.

95. Lam FMH, Bui M, Yang FZH, Pang MYC. 2016 Chronic effects of stroke on hip bone density and tibial morphology: a longitudinal study. Osteoporos Int. *27*:591–603.

96. Lam FMH, Pang MYC. 2016 Correlation between tibial measurements using peripheral quantitative computed tomography and hip areal bone density measurements in ambulatory chronic stroke patients. Brain Inj. *30*:199–207.

97. MacIntyre NJ, Rombough R, Brouwer B. 2010 Relationships between calf muscle density and muscle strength, mobility and bone status in the stroke survivors with subacute and chronic lower limb hemiparesis. J Musculoskelet Neuronal Interact. *10*:249–255.

98. Pang MYC, Ashe MC, Eng JJ. 2007 Muscle weakness, spasticity and disuse contribute to demineralization and geometric changes in the radius following chronic stroke. Osteoporos Int. *18*:1243–1252.

99. Shields RK, Dudley-Javoroski S, Boaldin KM, Corey TA, Fog DB, Ruen JM. 2006 Peripheral Quantitative Computed Tomography: Measurement Sensitivity in Persons With and Without Spinal Cord Injury. Arch Phys Med Rehabil. *87*:1376–1381.

100. Talla R, Galea M, Lythgo N, Angeli T, Eser P. 2011 Contralateral comparison of bone geometry, BMD and muscle function in the lower leg and forearm after stroke. J Musculoskelet Neuronal Interact. *11*:306–313.

101. Ward KA, Adams JE, Hangartner TN. 2005 Recommendations for thresholds for cortical bone geometry and density measurement by peripheral quantitative computed tomography. Calcif Tissue Int. *77*:275–280.

102. Hangartner TN, Short DF. 2007 Accurate quantification of width and density of bone structures by computed tomography. Med Phys. *34*:3777–3784.

103. Coupaud S, Jack LP, Hunt KJ, Allan DB. 2009 Muscle and bone adaptations after treadmill training in incomplete Spinal Cord Injury: a case study using peripheral Quantitative Computed Tomography. J Musculoskelet Neuronal Interact. *9*:288–297.

104. Duckham RL, Frank AW, Johnston JD, Olszynski WP, Kontulainen SA. 2013 Monitoring time interval for pQCT-derived bone outcomes in postmenopausal women. Osteoporos Int. *24*:1917–1922.

105. Groll O, Lochmüller EM, Bachmeier M, Willnecker J, Eckstein F. 1999 Precision and intersite correlation of bone densitometry at the radius, tibia and femur with peripheral quantitative CT. Skeletal Radiol. *28*:696–702.

106. Rinaldi G, Wisniewski CA, Setty NG, Leboff MS. 2011 Peripheral quantitative computed tomography: optimization of reproducibility measures of bone density, geometry, and strength at the radius and tibia. J Clin Densitom. *14*:367–373.

107. Swinford RR, Warden SJ. 2010 Factors affecting short-term precision of musculoskeletal measures using peripheral quantitative computed tomography (pQCT). Osteoporos Int. *21*:1863–1870.

108. Veitch SW, Findlay SC, Ingle BM, *et al.* 2004 Accuracy and precision of peripheral quantitative computed tomography measurements at the tibial metaphysis. J Clin Densitom. *7*:209–217.

109. Belavy DL, Beller G, Ritter Z, Felsenberg D. 2011 Bone structure and density via HR-pQCT in 60d bed-rest, 2-years recovery with and without countermeasures. J Musculoskelet Neuronal Interact. *11*:215–226.

110. Burrows M, Cooper DML, Liu D, McKay HA. 2009 Bone and muscle parameters of the tibia: agreement between the XCT 2000 and XCT 3000 instruments. J Clin Densitom. *12*:186–194.

111. Koenig C, Wey H, Binkley T. 2008 Precision of the XCT 3000 and comparison of densitometric measurements in distal radius scans between XCT 3000 and XCT 2000 peripheral quantitative computed tomography scanners. J Clin Densitom. *11*:575–580.

112. Sherk VD, Thiebaud RS, Chen Z, Karabulut M, Kim SJ, Bemben DA. 2014 Associations between pQCT-based fat and muscle area and density and DXA-based total and leg soft tissue mass in healthy women and men. J Musculoskelet Neuronal Interact. *14*:411–417.

113. Marjanovic EJ, Ward KA, Adams JE. 2009 The impact of accurate positioning on measurements made by peripheral QCT in the distal radius. Osteoporos Int. *20*:1207–1214.

114. Sun L, Beller G, Felsenberg D. 2009 Quantification of bone mineral density precision according to repositioning errors in peripheral quantitative computed tomography (pQCT) at the radius and tibia. J Musculoskelet Neuronal Interact. *9*:18–24.

115. Genant HK, Guglielmi G, Jergas M eds. 1998 Bone Densitometry and Osteoporosis . Springer Berlin Heidelberg, Berlin.

116. MacIntyre NJ. 1999 In Vivo Assessment of the Relation between Trabecular Bone Structure in the Radius and Gender, Aging, Mechanical Loading and Fracture . McMaster University, Hamilton, Ontario, Canada. Available at: http://hdl.handle.net/11375/6512.

117. Lala D, Cheung AM, Lynch CL, *et al.* 2014 Measuring apparent trabecular structure with pQCT: a comparison with HR-pQCT. J Clin Densitom. *17*:47–53.

118. Rittweger J, Michaelis I, Giehl M, Wüsecke P, Felsenberg D. 2004 Adjusting for the partial volume effect in cortical bone analyses of pQCT images. J Musculoskelet Neuronal Interact. *4*:436–441.

119. Prevrhal S, Engelke K, Kalender WA. 1999 Accuracy limits for the determination of cortical width and density: the influence of object size and CT imaging parameters. Phys Med Biol. *44*:751–764.

120. Wong AKO, Beattie KA, Min KKH, *et al.* 2015 A trimodality comparison of volumetric bone imaging technologies. Part I: Short-term precision and validity. J Clin Densitom. *18*:124–135.

121. Wong AKO, Beattie KA, Min KKH, *et al.* 2015 A Trimodality Comparison of Volumetric Bone Imaging Technologies. Part III: SD, SEE, LSC Association With Fragility Fractures. J Clin Densitom. *18*:408–418.

122. Stratec. 2004 XCT 2000 Manual Software Version 5.50.

123. Stratec. 2004 XCT Research Series Manual Software. Version 5.50.

124. Ashe MC, Khan KM, Kontulainen SA, *et al.* 2006 Accuracy of pQCT for evaluating the aged human radius: an ashing, histomorphometry and failure load investigation. Osteoporos Int. *17*:1241–1251.

125. Kontulainen S, Liu D, Manske S, Jamieson M, Sievänen H, McKay H. 2007 Analyzing cortical bone cross-sectional geometry by peripheral QCT: comparison with bone histomorphometry. J Clin Densitom. *10*:86–92.

126. Cervinka T, Rittweger J, Hyttinen J, Felsenberg D, Sievänen H. 2011 Anatomical sector analysis of load-bearing tibial bone structure during 90-day bed rest and 1-year recovery. Clin Physiol Funct Imaging. *31*:249–257.

127. Hangartner TN. 2007 Thresholding technique for accurate analysis of density and geometry in QCT, pQCT and microCT images. J Musculoskelet Neuronal Interact. *7*:9–16.

128. Cervinka T, Giangregorio L, Lala D, *et al.* 2014 New Tool for Accurate Certical Boone Analysis in pQCT Images. J Bone Miner Res. *29*:222–222.

129. Krug R, Burghardt AJ, Majumdar S, Link TM. 2010 High-resolution imaging techniques for the assessment of osteoporosis. Radiol Clin North Am. *48*:601–621.

130. Gordon CL, Webber CE, Adachi JD, Christoforou N. 1996 In vivo assessment of trabecular bone structure at the distal radius from high-resolution computed tomography images. Phys Med Biol. *41*:495–508.

131. Cervinka T, Sievänen H, Lala D, Cheung AM, Giangregorio L, Hyttinen J. 2015 A new algorithm to improve assessment of cortical bone geometry in pQCT. Bone. *81*:721–730.

132. Cervinka T, Hyttinen J, Sievänen H. 2012 Threshold-free automatic detection of cortical bone geometry by peripheral quantitative computed tomography. J Clin Densitom. *15*:413–421.

133. Wong AKO, Beattie KA, Min KKH, *et al.* 2015 A Trimodality Comparison of Volumetric Bone Imaging Technologies. Part II: 1-Yr Change, Long-Term Precision, and Least Significant Change. J Clin Densitom. *18*:260–269.

134. Cervinka T, Sievänen H, Hyttinen J, Rittweger J. 2014 Bone loss patterns in cortical, subcortical, and trabecular compartments during simulated microgravity. J Appl Physiol. *117*:80–88.

135. Rantalainen T, Nikander R, Heinonen A, Daly RM, Sievanen H. 2011 An open source approach for regional cortical bone mineral density analysis. J Musculoskelet Neuronal Interact. *11*:243–248.

136. Rantalainen T, Nikander R, Daly RM, Heinonen A, Sievänen H. 2011 Exercise loading and cortical bone distribution at the tibial shaft. Bone. *48*:786–791.

137. Kazakia GJ, Tjong W, Nirody JA, *et al.* 2014 The influence of disuse on bone microstructure and mechanics assessed by HR-pQCT. Bone. *63*:132–140.

138. Rantalainen T, Nikander R, Heinonen A, Suominen H, Sievänen H. 2010 Direction-specific diaphyseal geometry and mineral mass distribution of tibia and fibula: a pQCT study of female athletes representing different exercise loading types. Calcif Tissue Int. *86*:447–454.

139. Evans RK, Negus CH, Centi AJ, Spiering BA, Kraemer WJ, Nindl BC. 2012 Peripheral QCT sector analysis reveals early exercise-induced increases in tibial bone mineral density. J Musculoskelet Neuronal Interact. *12*:155–164.

140. Kontulainen SA, Johnston JD, Liu D, Leung C, Oxland TR, McKay HA. 2008 Strength indices from pQCT imaging predict up to 85% of variance in bone failure properties at tibial epiphysis and diaphysis. J Musculoskelet Neuronal Interact. *8*:401–409.

141. Lochmüller E-M, Lill CA, Kuhn V, Schneider E, Eckstein F. 2002 Radius bone strength in bending, compression, and falling and its correlation with clinical densitometry at multiple sites. J Bone Miner Res. *17*:1629–1638.

142. MacIntyre NJ, Adachi JD, Webber CE. 2003 In vivo measurement of apparent trabecular bone structure of the radius in women with low bone density discriminates patients with recent wrist fracture from those without fracture. J Clin Densitom. *6*:35–43.

143. Jamal SA, Gilbert J, Gordon C, Bauer DC. 2006 Cortical pQCT measures are associated with fractures in dialysis patients. J Bone Miner Res. *21*:543–548.

144. Engelke K, Lang T, Khosla S, *et al.* 2015 Clinical Use of Quantitative Computed Tomography (QCT) of the Hip in the Management of Osteoporosis in Adults: the 2015 ISCD Official Positions-Part I. J Clin Densitom. *18*:338–358.

145. Dodds RA, Emery RJ, Klenerman L, Chayen J, Bitensky L. 1989 Comparative metabolic enzymatic activity in trabecular as against cortical osteoblasts. Bone. *10*:251–254.

146. Reina P, Cointry GR, Nocciolino L, *et al.* 2015 Analysis of the independent power of age-related, anthropometric and mechanical factors as determinants of the structure of radius and tibia in normal adults. A pQCT study. J Musculoskelet Neuronal Interact. *15*:10–22.

147. Rittweger J, Beller G, Ehrig J, *et al.* 2000 Bone-muscle strength indices for the human lower leg. Bone. *27*:319–326.

148. Capozza RF, Feldman S, Mortarino P, *et al.* 2010 Structural analysis of the human tibia by tomographic (pQCT) serial scans. J Anat. *216*:470–481.

149. Morse LR, Battaglino RA, Stolzmann KL, *et al.* 2009 Osteoporotic fractures and hospitalization risk in chronic spinal cord injury. Osteoporos Int. *20*:385–392.

150. Fattal C, Mariano-Goulart D, Thomas E, Rouays-Mabit H, Verollet C, Maimoun L. 2011 Osteoporosis in persons with spinal cord injury: the need for a targeted therapeutic education. Arch Phys Med Rehabil. *92*:59–67.

Figure captions:

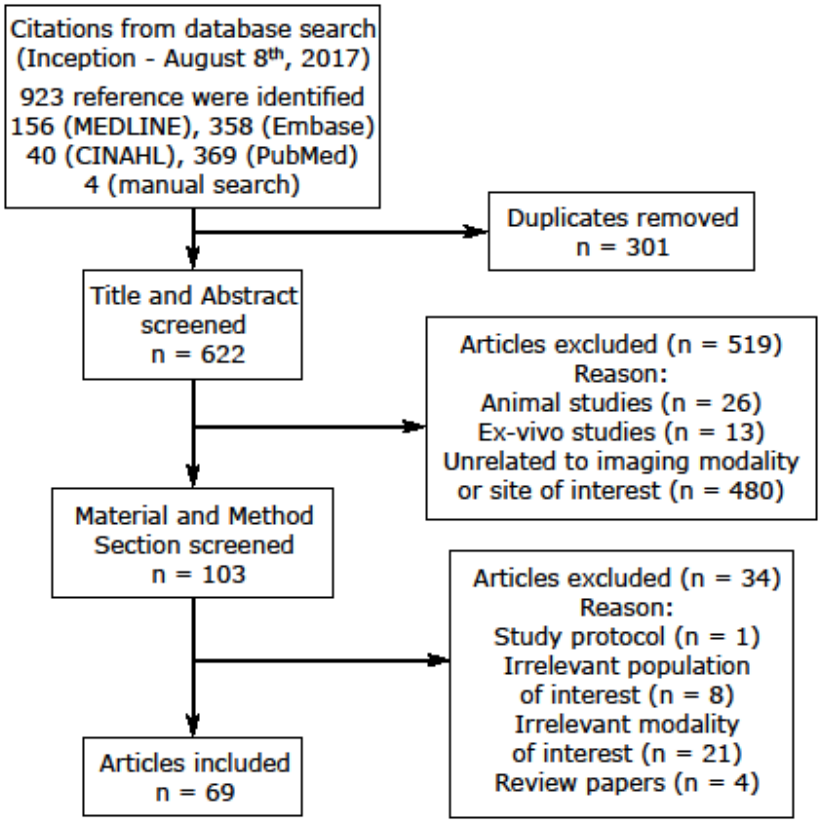

Figure 1: PRISMA flow chart for article inclusion process.

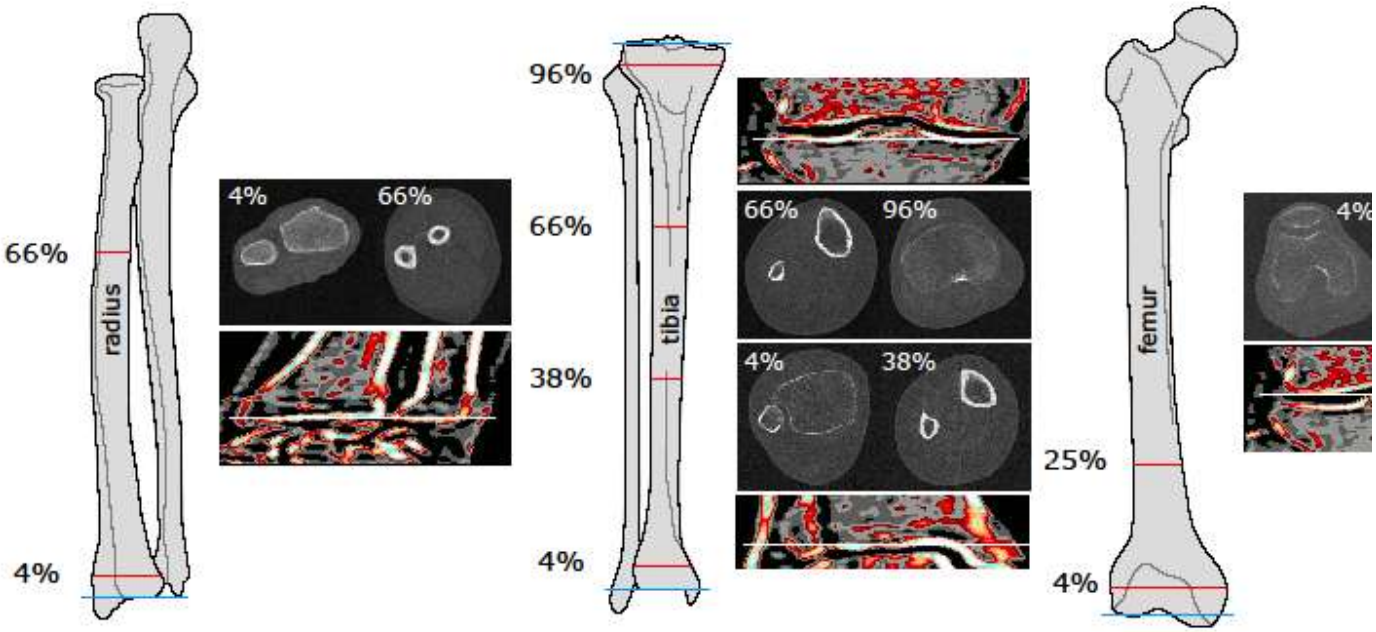

Figure 2: Imaging site recommended by Stratec for various long bones. Blue lines depict locations of the reference lines, red lines depict location of particular imaging sites. Detailed images and scout scans are on the right.

Table 1: Imaging modalities included in the literature review

Technology	Scanner	Number of publications	Study
Single-slice	XCT 2000	20	(26,47,48,57,58,60,64,66,71,73–75,77,78,80,85,86,88,90,98–100)
	XCT 3000	34	(28,30,31,39,40,49–56,61,63,65,67–72,76,81–84,87,89–96)
	XCT 960	2	(32,38)
	OsteoQuant©	1	(46)
Multi-slice	XtremeCT	2	(41,42)
	Densiscan 2000	2	(29,45)
	Densiscan 1000	2	(43,44)

Note: In studies Sherk et al. [59], Gibbons et al. [62] and Dudley-Javoroski and Shields [37], the authors did not report which type of XCT scanner they used and in study Dudley-Javoroski and Shields [71] the authors used both XCT 2000 and 3000 scanners.

Table 2: Technical specifications of the Stratec 2000/3000 peripheral QCT scanners

Scanner	Dimensions (l/w/h) [cm]	Weight [kg]	Distance of travel [cm]	Gantry opening [cm]	Scanning time* [s]	Voxel size [mm]	Slice thickness [mm]	Radiation dose [mSv]
XCT 2000	128 x 55 x 62	45	40	14	90	0.1 - 1.0	0.5 - 2.0	< 0.001
XCT 3000	128 x74 x91	90	40	30	90	0.2 - 1.0	2.0 - 2.5	< 0.001

*actual scanning times depend on scan parameters (e.g., size of imaged object and scanning speed) and whether or not a scout scan is done

Table 3: Imaging sites reported and the clinical rationale for their inclusion

Bone	Site	Rationale
Radius	4%	Predominantly trabecular bone, this compartment has higher metabolic activity per unit mass, in contrast to the cortical compartment located at shafts of long bones [145]
	20%	Standard imaging location to assess cortical bone for older XCT 960 scanner [32,38]
	30/33%	Anatomical proximity to the origin/insertion of many muscle groups (e.g., Abductor pollicis longus, extensor pollicis brevis and pronator teres) and a presumption of larger effects of muscles on cortical bone cross-sectional area at this site [66,98]
	65/66%	Largest muscle circumferences and muscle cross-sectional area [146]
Tibia	4/5%	Predominantly trabecular bone, this compartment has higher metabolic activity per unit mass, in contrast to the cortical compartment located at shafts of long bones [145]
	14%	vBMD and bending strength are the lowest in general population [85,147,148] suggesting a potential important correlation with fracture risk
	30/38%	Anatomical proximity to the origin/insertion of lower limb muscle groups (e.g., tibialis anterior, extensor hallucis longus, and soleus) and a presumption of larger effects of these muscles on cortical bone cross-sectional area at this site
	50%	Middle of the tibia shaft
	66%	Largest muscle circumferences and muscle cross-sectional area [146,147]
	85/86%	Presumably the most susceptible site to changes in the muscle-bone unit [30]
	95/96/98%	Predominantly trabecular bone, this compartment has higher metabolic activity per unit mass, in contrast to the cortical compartment located at shafts of long

		bones [145]
Femur	4%	Predominantly trabecular bone, this compartment has higher metabolic activity per unit mass, in contrast to the cortical compartment located at shafts of long bones [145]
	12/15%	Common fracture site [149,150]
	25%	Most proximal scan site due to insufficient hip abduction in patients with neurological impairments, absent or impaired lower extremity voluntary movement [31], and somewhat poorer image quality of more proximal sites [17].

Note, images from 25% site of the femur cannot typically be acquired by XCT 2000 in a majority of individuals due to small gantry opening; although it can often accommodate the limbs of individuals with neurologic impairment and significant atrophy. For healthy individuals with thigh circumferences (diameter > 14 cm) and long limbs, the XCT 3000 is required due to its larger gantry.

Table 4: Voxel sizes and slice thicknesses at various imaging sites reported in studies included in this review.

Bone	Site	N	Voxel size [mm]				Slice Thickness [mm]							Study
			0.5 x 0.5	0.4 x 0.4	0.3 x 0.3	0.2 x 0.2	2.5	2.4	2.3	2.2	2.1	2.0	1.0	
Radius	4%	12	x	x			x	x	x			x	x	(32,38,48,57,66–68,77,81–83,100)
	20%	2	x				x							(32,38)
	30%	2	x		x		x							(66,98)
	33%	3	x	x					x					(81,83,84)
	65/66%	4	x	x				x				x		(48,68,77,100)
Tibia	4/5%	34	x	x	x	x	x	x	x	x	x	x		(28,30,31,47–49,53–55,59,60,63,67,68,70–74,76–78,80,86,87,89,91,93–96,99,100,117)
	14%	6	x									x		(28,49,63,69,70,89)
	30%	1			x		x							(79)
	38%	26	x	x						x		x		(28,31,49,53–55,59,63,68–70,72,86,89,93,94)
	50%	2	x		x		x							(47,78)
	66%	24	x	x	x		x	x	x	x		x	x	(28,30,40,48,50,59,60,63–65,73–77,86,87,89,93,95–97,100)

	85/86%	3	x	x						x		x		(30,58,91)
	95/96/98%	8	x	x	x			x				x		(58,61,63,67,68,72,76,89)
Femur	4%	12		x	x			x		x		x		(28,31,51,53–55,61,67,68,72,89,93,94)
	12/15%	6	x							x		x		(30,51,52,58,90–92)
	25%	10			x							x		(28,31,53–55,72,89,93,94)

Table 5: Analysis protocols used in reviewed studies at the radius, tibia and femur

Site	Radius Protocol	N	Study	Tibia Protocol	N	Study
4%	CSAto/CSAt: C3P2 (130-400)	1	(66)	CSAto/CSAt: CxPx (200-400)	5	(30,71,86,91,99)
	CSAto/CSAt: C2P2 (169-400)	3	(81–83)	CSAto/CSAt: C3P2 (130-400)	2	(73,75)
	CSAto: C1P1 (280-45%)	1	(48)	CSAto/CSAt: C2P2 (169-400)	5	(78,80,87,95,96)
	CSAto: CxP1 (150-45%)	2	(67,68)	CSAto: C1P1 (169-45%)	1	(48)
	CSAto: CxP1 (180-45%)	1	(100)	CSAto: CxP1 (180-45%)	9	(31,54,67,68,72,89,93,94,100)
	CSAto: C1 (169)	1	(57)	CSAc: M4 (169-400)	1	(80)
	CSAc: M4 (169-710)	1	(66)	Osteo-Q architectural analysis	1	(73)
14%				CSAto: Cx (280)	1	(89)
30/33%	CSAto: C3P2()	1	(98)	CSAto: C3P2 (710-710)	1	(78)
	CSAc: M4 (710-710)	2	(66,98)	CSAc: M4 (710-710)	1	(78)
	CSAc: M1 (710)	3	(81,83,84)			
38%				CSAto: Mx (280)	7	(31,54,68,72,89,93,94)
				CSAc: Mx (710)	6	(31,54,68,72,93,94)
				CSAc: M1 (711)	1	(86)
50%				CSAto: C3P2 (710-710)	1	(78)
				CSAc: M4 (710-710)	1	(78)
65/66%	CSAto: Cx (280)	3	(67,68,100)	CSAto: M1 (280)	1	(48)
	CSAc: M1 (710)	1	(48)	CSAto: M1 (280)	1	(40)
	CSAc: Mx (710)	2	(67,68,100)	CSAto: Mx (280)	4	(30,68,93,100)
				CSAc: Mx (710)	4	(30,68,93,100)
				CSAc: M1 (710)	8	(48,64,73,75,86,87,95,96)

	CSAc: M4 (600-650)	1	(97)
85/86%	CSAto/CSAt: CxPx (200-400)	2	(30,91)
	CSAto/CSAt: CxP1 (120-650)	1	(58)
95/96%	CSAto: CxP1 (180-45%)	2	(61,72)
	CSAto: CxP1 (150-45%)	2	(67,89)
	CSAto: CxP1 (130-45%)	1	(68)
	CSAto/CSAt: CxP1 (120-650)	1	(58)

Table 5: Analysis protocols used in reviewed studies in various imaging sites of radius, tibia and femur (continued)

Site	Femur Protocol	N	Study
4%	CSAto/CSAt: CxP1 (120-650)	1	(58)
	CSAto: CxP1 (130-45%)	2	(67,89)
	CSAto: CxP1 (150-45%)	7	(31,54,61,68,72,93,94)
12%	CSAto/CSAt: CxPx (200-400)	4	(30,90–92)
	CSAto: CxP1 (200-45%)	1	(90)
15%	CSAto/CSAt: CxP1 (120-650)	1	(58)
25%	CSAto: Mx (280)	7	(31,54,68,72,89,93,94)
	CSAc: Mx (710)	7	(31,54,68,72,89,93,94)

x denotes unknown number of contour (C) or peel (P) mode (M), CSAto – total cross-sectiona area, CSAc – cortical cross-sectional area, CSAt – trabecular cross-sectional area, N – number of studies

Table 6: Key bone traits.

Scanner	Imaging site	Observational studies	Intervention studies	Fracture risk prediction and bone strength traits
pQCT	Epiphysis	BMCto	BMCto	BMDt
		BMDt	BMDt	BSI

	Diaphysis	BMCto	BMCto	PMI
		BMCc	BMCc	SSI
		CSAc	CoTh	
		CoTh		

BMCto – total bone mineral content, BMCc – cortical bone mineral content, BMDt – trabecular bone mineral density, CSAc – cortical cross-sectional area, CoTh – cortical thickness, BSI – bone strength index (resistivity in compression), PMI – polar moment of inertia (resistivity in torsion), SSI – stress strain index (resistivity in bending).

Table 7: Precision and least significant changes of key traits for particular bones and sites as measured by Stratec pQCT [17,31,73,81,83,95,104–108]

Radius				Tibia				Femur			
Site	Trait	$CV_{\%RMS}$ [%]	LSC [%]	Site	Trait	$CV_{\%RMS}$ [%]	LSC [%]	Site	Trait	$CV_{\%RMS}$ [%]	LSC [%]
4%	BMCto	3.0	8.3	4%	BMCto	1.0	2.7	4%	BMCto	1.1	3.0
	BMDto	3.9	10.8		BMDto	1.3	3.5		BMDto	2.0	5.7
	BMCt	4.7	13.0		BMCt	2.1	5.8		BMCt	-	-
	BMDt	2.1	5.8		BMDt	1.1	3.2		BMDt	2.3	6.2
	BSI	5.4	15.0		BSI	2.0	5.5		BSI	6.0	16.6
33%	BMCto	2.5	6.9	38%	BMCto	0.6	1.6	25%	BMCto	2.0	5.6
	BMCc	0.8	2.2		BMCc	0.9	2.5		BMCc	2.6	7.2
	CSAc	1.8	4.9		CSAc	1.1	3.1		CSAc	2.9	8.0
	CoTh	1.6	4.3		CoTh	1.2	3.3		CoTh	3.6	10.0
	PMI	2.2	6.1		PMI	2.0	5.4		PMI	1.7	4.7
	SSI	2.1	5.8		SSI	1.6	4.5		SSI	4.1	11.2
66%	BMCto	-	-	66%	BMCto	0.8	2.1				
	BMCc	3.4	9.5		BMCc	0.9	2.5				
	CSAc	3.1	8.6		CSAc	1.1	3.0				
	CoTh	-	-		CoTh	1.4	3.8				
	PMI	-	-		PMI	1.4	3.8				
	SSI	4.0	11.1		SSI	1.8	4.9				
				96%	BMCto	3.5	9.7				
					BMDto	3.1	8.6				
					BMCt	-	-				
					BMDt	2.1	5.8				
					BSI	-	-				

BMCto – total bone mineral content, BMCc – cortical bone mineral content, BMCt – trabecular bone mineral content, BMDto – total bone mineral density, BMDt – trabecular bone mineral density, CSAc – cortical cross-sectional area, CoTh – cortical thickness, BSI – bone strength index (resistivity in compression), PMI – polar moment of inertia (resistivity in bending), SSI – stress strain index (resistivity in bending), $CV_{\%RMS}$ – relative coefficient of variation (short-term precision), LSC – least significant change. The clinimetric properties (the precision and least significant changes) for selected bone were abstracted from the available literature known to authors using the same imaging sites described in this review. Where feasible, the $CV_{\%RMS}$ and LSC were calculated from the available published data as $CV_{\%RMS}$ = LSC/2.77 and LSC = 2.77*$CV_{\%RMS}$, respectively.

Table 8: Recommendations for minimal image acquisition protocols for clinical and research settings using Stratec pQCT scanners.

Setting	Region of interest	Length measurement	Reference line placement	Imaging sites	Voxel size [mm]	Slice thickness [mm]
Research Settings (Humans)	Radius	Measure from the medial aspect of the styloid process to the humero-radial joint cleft	Place at the superior aspect of the cortical shell at the most distal and flattest portion of the plateau of the endplate	4%	0.4 x 0.4	2 – 2.5
				66%	0.5 x 0.5	
	Tibia	Measure from the most distal palpable end of the medial malleolus to the most proximal edge of the medial tibial plateau (the medial join cleft)		4%	0.4 x 0.4	
				38%	0.5 x 0.5	
				66%	0.5 x 0.5	
	Femur	Measure from the most distal limit of the lateral femoral condyle to the most proximal palpable limit of the greater trochanter	Place at the distal limit of the lateral femoral condyle	4%	0.3 x 0.3	
				25%	0.5 x 0.5	

Clinical Practice Settings	Tibia	Measure from the most distal palpable end of the medial malleolus to the most proximal edge of the medial tibial plateau (the medial join cleft)	Place at the superior aspect of the cortical shell at the most distal and flattest portion of the plateau of the endplate	4% 38% 66%	0.4 x 0.4 0.5 x 0.5 0.5 x 0.5	2 – 2.5